

Dynamical microscopic three-cluster description of ${}^6\text{Li}$

A. Csóttó and R. G. Lovas

Institute of Nuclear Research of the Hungarian Academy of Sciences (ATOMKI), Debrecen, H-4001, Hungary

(Received 13 January 1992)

We have implemented a dynamical microscopic $\alpha + p + n$ model for the description of the ground state (g.s.) of ${}^6\text{Li}$ in an attempt to achieve the perfection of macroscopic $\alpha + p + n$ three-body models. We use a generator-coordinate approach, which includes $(pn)\alpha$, $(\alpha n)p$, and $(\alpha p)n$ partitions with all angular-momentum components of any significance. The trial function is constructed out of $0s$ and a set of $0s$, $0p$, $0d$ harmonic-oscillator (h.o.) eigenfunctions of the α intrinsic and of intercluster Jacobi coordinates, respectively, with the generator coordinates being the h.o. size parameters. The effective nucleon-nucleon force used contains tensor and spin-orbit terms. We have determined its parameters by fitting to the properties of the subsystems. We found that the description of the subsystems is less perfect than with central forces, and explained this by the inconsistency of the use of a tensor force with describing the α g.s. by $0s$ oscillator states. The binding of ${}^6\text{Li}$ with this force was found to be about 1 MeV too weak. After readjusting the force to yield the correct energy, we calculated some properties of ${}^6\text{Li}$. The radius obtained is somewhat too large, and the tiny quadrupole moment has the wrong sign. The results for the weights of the components of summed nucleon spin and orbital momentum $(S, L) = (1, 0)$, $(1, 1)$, $(1, 2)$, and $(0, 1)$ are 94.6%, 0.2%, 3.9%, and 1.3%, respectively. The $(1, 2)$ component comes predominantly from clusterization $(pn)\alpha$; the others can be attributed to any of the highly overlapping partitions. The $\alpha + d$ and ${}^5\text{He} + p$ spectroscopic factors were calculated with a new formula, which expresses them in the generator-coordinate basis directly, without resort to integral transformations. The estimates for the $\alpha + d$ spectroscopic factor, ~ 0.9 , are realistic, but those for ${}^5\text{He} + p$ are a factor of 2 too high. This is understood to be a consequence of the model's tendency to compress the low-energy continuum, which appears to be a general defect of forces that are constrained to reproduce the bulk properties of the α particle in terms of $0s$ states. Thus a radical remedy would require an improvement of the description of the cluster internal motion.

PACS numbers: 21.60.Gx, 21.10.Jx, 27.20.+n

I. INTRODUCTION

All bound or scattered few-nucleon systems tend to be clustered strongly [1]. Strong clustering implies that the behavior of the system is primarily determined by the motion of the clusters relative to each other, and that renders both the microscopic and macroscopic cluster models of such systems realistic.

In the microscopic models all nucleonic degrees of freedom are treated explicitly, and the nucleons are usually assumed to interact via a two-body force. The cluster internal motions are mostly described by simple harmonic-oscillator (h.o.) configurations, and the Pauli principle is taken into account exactly. The basic version of the microscopic model assumes that the system is partitioned into two clusters. Refinements either include further configurations (other cluster partitions [2] or excited clusters [3]) or allow a cluster to split into two clusters [2], which move subject to some constraint.

The macroscopic approach [4] neglects the internal structure of the clusters except for a phenomenological treatment of the Pauli principle, and uses phenomenological two-body intercluster potentials. At the expense of this simplification, however, it is able to treat the relative motion of three clusters with the rigor of few-body physics [5].

The reduction of the microscopic cluster approach to the macroscopic description is a nice example for the reduction problem in few-body physics. Unlike the quark level of description, these two levels are still within the realm of nonrelativistic quantum mechanics, thus their relationship can be elaborated thoroughly.

In this paper we wish to examine, through one example, to what extent the two approaches correspond to each other. To this end we present dynamical microscopic three-cluster calculations that treat the intercluster dynamics with an accuracy comparable with that of existing macroscopic three-body calculations. We consider the ground state (g.s.) of ${}^6\text{Li}$ as composed of $\alpha + p + n$ [6], which is the simplest three-cluster system. Our work has been prompted by the controversial results produced by microscopic [7–10] and macroscopic [11–17] models.

Our earlier model [7–10] of ${}^6\text{Li}$ can be regarded as an $\alpha + (p + n)$ three-cluster microscopic model in which the summed nucleon spin is constrained to $S = 1$ and the relative orbital momenta between p and n (l_1) and between (pn) and α (l_2) to $l_1 = l_2 = 0$ (and thus the total orbital momentum to $L=0$). Though all these calculations reproduce the electromagnetic properties reasonably [18–20], there is a significant discrepancy between them in the spectroscopic factors of deuteron and proton removal ($s^{d\alpha}$ and $s^{5\text{He}p}$). While the discrepancy in $s^{d\alpha}$

seems to be accounted for by Pauli effects neglected in the macroscopic models [21], the disagreement in $s^5\text{He}p$ is too large for that. Moreover, experiment supports the macroscopic model in that respect [17].

The logic of the paper is as follows. To outline our approach, we shall first specify the model state space used in the description of ${}^6\text{Li}$ (Sec. II). In accord with the usual philosophy of the few-body approach, we choose an interaction (Sec. III) that is optimized to describe the two-body (two-cluster) subsystems in state spaces comparable with those to be used for $\alpha + p + n$ (Sec. III A). The first test of the approach is to see how well this reproduces the ${}^6\text{Li}$ energy (Sec. III B). We shall elaborate further on the physical properties of ${}^6\text{Li}$ in Sec. IV. After a brief diversion to the problem of the quadrupole moment (Sec. IV A), we shall examine in detail the ingredients of the model wave function and its predictions for the fragmentation properties. The ingredients of the model ${}^6\text{Li}$ will be analyzed energetically as well as directly in terms of the weights of the various components in the wave function (Sec. IV B). This gives an opportunity to make a comparison with previous microscopic and macroscopic descriptions and to assess the significance of the different segments of the state space. We find a non-negligible difference between the macroscopic and microscopic models in the $S = 0, L = 1$ component. Therefore, in comparing the predictions for the spectroscopic factors (Sec. IV C), we shall examine the role of this component. We shall see that, in fact, the discord in the weights cannot account for the discrepancy found in the spectroscopic factors. We thus have to conclude (Sec. V) that the cause of the discrepancy is more fundamental, and its existence points to a limitation of the few-cluster approach that involves a schematic description of the cluster intrinsic states.

Some formulae for the weights ("amounts") of clustering and a new method for the calculation of the spectroscopic factors are presented in the Appendices.

II. MODEL

We have set up a microscopic multiconfiguration multicluster formalism, similar in many respects to earlier ones [22]. This is combined with a variational approximation to the A -particle problem. Our trial function is a sum over various cluster arrangements, each associated with a particular set of intercluster Jacobi coordinates. A general term in the model of ${}^6\text{Li}$ has the form

$$\Psi_{S,(l_1 l_2)L}^{(12)3} = \mathcal{A} \left\{ \left[\Phi_S [\chi_{l_1}^{12}(\rho_1) \chi_{l_2}^{(12)3}(\rho_2)] \right]_{JM} \right\}, \quad (1)$$

where 1, 2, 3 in the superscripts are elements of any one of the permutations of the labels α, p, n ; \mathcal{A} is the intercluster antisymmetrizer [23]; $\Phi_{SM_S} = [(\Phi^1 \Phi^2) \Phi^3]_{SM_S}$ is composed of the cluster intrinsic wave functions Φ^i ; the $\chi(\rho)$ are functions of the intercluster Jacobi coordinates

$$\rho_1 = \mathbf{r}_2 - \mathbf{r}_1, \quad (2a)$$

$$\rho_2 = \mathbf{r}_3 - \frac{m_1 \mathbf{r}_1 + m_2 \mathbf{r}_2}{m_1 + m_2} \quad (2b)$$

(m_i are the cluster masses); and $[]_{jm}$ denotes angular-

momentum coupling. While the internal wave functions Φ^p and Φ^n are just spin-isospin eigenstates, the function Φ^α is

$$\Phi^\alpha = \sum_i^{N_\alpha} c_i \phi_{\beta_i}, \quad (3)$$

where ϕ_{β_i} are h.o. Slater determinants, of different size parameters β_i , each projected onto the 0s h.o. wave function describing the respective zero-point vibration of the α center of mass. (The spatial factor of such a ϕ_{β_i} is equal to a product of 0s h.o. functions of three intrinsic Jacobi coordinates.) To correspond to the macroscopic models, this combination should describe the α g.s. The coefficients of combination can be obtained by a diagonalization of the α intrinsic Hamiltonian in the space of the center-of-mass-projected Slater determinants. The intercluster functions $\chi_{lm}(\rho_i)$ are expanded as

$$\chi_{lm}(\rho_i) = \sum_k^{N_i} C_k \Gamma_{kl}^{(i)}(\rho_i), \quad (4)$$

with $\Gamma_{kl}^{(i)}$ being h.o. eigenfunctions of radial node number zero,

$$\Gamma_{kl}^{(i)}(\rho_i) \propto \rho_i^l \exp(-\frac{1}{2} \gamma_{ik} \rho_i^2) Y_{lm}(\hat{\rho}_i). \quad (5)$$

The matrix elements involving the basis functions are expressed as integral transforms of matrix elements of Slater determinants, of shifted Gaussians, projected to total momentum zero. One can derive such a relationship by using the fact [24–26] that, apart from a trivial factor, a shifted Gaussian is the generating function of the h.o. eigenfunctions.

We thus describe ${}^6\text{Li}$ as a superposition of the three arrangements, $(pn)\alpha$, $(\alpha p)n$, $(\alpha n)p$, with the α particle constrained to be in a spin-isospin zero state. From among the $[S, (l_1, l_2)L]J$ values adding up to $J^\pi = 1^+$, we include those with $S = 0, 1, L = 0, 1, 2$ with at most one of the l_i exceeding 1. The various arrangements of the same S, L are highly nonorthogonal because of the completeness of a basis of each arrangement by itself and, in addition, because of antisymmetrization. We therefore truncate the basis in the different arrangements in a complementary manner. The sets of $[S, (l_1, l_2)L]J$ that are clearly favored energetically in one or two of the arrangements, are only kept in those particular arrangements. The trial function is thus composed of terms $\Psi_{S,(l_1 l_2)L}^{(12)3}$ of the following types:

$$\begin{aligned} \Psi^{\alpha pn} = & \Psi_{1,(00)0}^{(pn)\alpha} + \Psi_{1,(20)2}^{(pn)\alpha} + \Psi_{1,(02)2}^{(pn)\alpha} + \Psi_{0,(11)1}^{(pn)\alpha} \\ & + \Psi_{1,(11)0}^{(\alpha p)n} + \Psi_{1,(11)1}^{(\alpha p)n} + \Psi_{1,(11)2}^{(\alpha p)n} + \Psi_{0,(11)1}^{(\alpha p)n} \\ & + \Psi_{1,(11)0}^{(\alpha n)p} + \Psi_{1,(11)1}^{(\alpha n)p} + \Psi_{1,(11)2}^{(\alpha n)p} + \Psi_{0,(11)1}^{(\alpha n)p}. \end{aligned} \quad (6)$$

This basis incorporates all microscopic bases of the form of $\alpha + d$, $\alpha + p + n$, ${}^5\text{He} + p$, and ${}^5\text{Li} + n$ used previously in Refs. [2, 27], and, in the relative-motion space, it is more extensive than the variational macroscopic bases [15]. The model is more restrictive than the Faddeev mod-

els [5, 11–13] only in the spatial region of three-particle breakup, which is not expected to play any role in the g.s.

Moreover, our formalism allows to include, in addition to the α g.s. (α_0), the first few breathing modes $\alpha_1, \alpha_2, \dots$:

$$\Psi = \Psi^{\alpha_0 pn} + \Psi^{\alpha_1 pn} + \dots \quad (7)$$

The breathing modes are obtained as the excited states in the diagonalization that produces the α g.s. The excitation of the breathing modes in the composite system allows for the distortion of the α cluster in the vicinity of the others. The model may hereby include the state spaces of the α -distortion models [3, 7–10] as well.

We had to compromise on the basis to limit its size and to avoid numerical instabilities arising from its being close to linear dependence. We had to omit the two clusterizations that proved the least significant energetically: $\{(pn)\alpha; S, (l_1 l_2)L=1, (02)2\}$ and $\{(\alpha p)n; S, (l_1 l_2)L=1, (11)1\}$. In test calculations the weights of these terms were found to be less than 0.2% each. The sets $\{\beta_i\}$, $\{\gamma_{1i}\}$, $\{\gamma_{2i}\}$, which can be regarded as discretized values of some generator coordinates β , γ_1 , γ_2 , had also to be restricted. The α , relative pn , and all other relative-motion bases were chosen to have dimensions 2, 9, and 6, respectively. The β and $\gamma_{(pn)}$ values were determined by minimization of the α and d energies, while the other γ values were taken from Kukulin *et al.* [15], who used such bases in a macroscopic $\alpha + p + n$ model for the $(pn) + \alpha$ relative motion. Test calculations show that a three-dimensional α basis (optimized) would only yield 0.005 and 0.02 MeV lower α and ${}^6\text{Li}$ energy, respectively, than the two-dimensional one. The dimension 9 for $\gamma_{(pn)}$ seems unnecessarily high (for the deuteron we had found 5 to be adequate [9]); nevertheless, we kept this high value because we wanted to conform to the calculations of Kukulin *et al.* [15]. The values of the sets of β and γ are given in Table I.

We describe the two-cluster subsystems analogously. In keeping with (1), we define

$$\Phi_{(12)[(S_1 l_1) I_1]} = \mathcal{A} \left\{ [\phi_{(12)(S_1)} \tilde{\chi}_{l_1}^{12}(\rho_1)]_{I_1 M_1} \right\}, \quad (8)$$

where $\phi_{(12)(S_1 M_{S_1})} = [\Phi^1 \Phi^2]_{S_1 M_{S_1}}$. The wave function of the deuteron involves summation over S_1 ,

$$\Phi_d = \Phi_{(pn)[(10)1]} + \Phi_{(pn)[(12)1]}, \quad (9)$$

whereas the five-nucleon wave functions involve summation over the α states, e.g.,

$$\Phi_{\alpha n} = \Phi_{(\alpha_0 n)[(\frac{1}{2} l_1) I_1]} + \Phi_{(\alpha_1 n)[(\frac{1}{2} l_1) I_1]}. \quad (10)$$

Unless stated otherwise, the parameters of the subsystem bases correspond strictly to those of the three-cluster basis.

III. INTERACTION

If the dynamics contained in the macroscopic $\alpha + p + n$ calculations has anything to do with the actual six-

nucleon system, it must be derivable from a microscopic picture. Since even a structureless α particle seems a realistic assumption, one expects that it suffices for the underlying microscopic model to be sketchy for the α particle. It must, however, depict the relative motion faithfully. It is thus reasonable to assume that there exists a nucleon-nucleon interaction that is appropriate for the α cluster in a truncated subspace and, at the same time, for the $\alpha + p$, $\alpha + n$, and $p + n$ systems in the full state spaces of these relative motions. To produce realistic results even in the minute admixtures with $(S, L) \neq (1, 0)$, this interaction has to contain tensor and spin-orbit terms as well. We have chosen the form

$$\begin{aligned} V_{12}(r) = & (W + MP^r + BP^\sigma - HP^\tau) \sum_{i=1,2} V_i e^{-r^2/a_i^2} \\ & + (W_T + M_T P^r) r^2 \\ & \times \sum_{i=3,4} V_i e^{-r^2/a_i^2} [3(\sigma_1 \mathbf{r})(\sigma_2 \mathbf{r})/r^2 - \sigma_1 \sigma_2] \\ & + V_5 e^{-r^2/a_5^2} \hbar^{-2} \mathbf{l}(\sigma_1 + \sigma_2), \end{aligned} \quad (11)$$

where P are the space-, spin-, and isospin-exchange operators, $W + M + B + H = 1$, $W_T + M_T = 1$, $\mathbf{r} = \mathbf{r}_2 - \mathbf{r}_1$, σ_i are the Pauli vectors of the nucleonic spin, and

$$\mathbf{l} = -\frac{i}{2} \hbar \mathbf{r} \times (\nabla_2 - \nabla_1) \quad (12)$$

is the orbital momentum of the relative motion of the two nucleons.

We adopted one of the spin-orbit interactions of Ref. [28] and constructed the central and tensor parts step by step drawing on the fact that the dynamics of some of the subsystems only contains certain combinations of the force terms [9], but all subsystems together contain all parameters.

Since our present formalism has been put onto a computer for only bound states for the time being, in describing the scattering states of the subsystems $\alpha + p$, $\alpha + n$, and $p + n$ we used the traditional generator-coordinate scattering formalism, in which the relative motion is described by a combination of angular-momentum projected shifted Gaussians [10].

A. Description of subsystems

In the search for the force parameters the free clusters d , t , and α were described by superpositions of intrinsic $0s$ h.o. states ϕ_β , of different size parameters β . These expansions were similar to Eq. (3), but here the bases were chosen large to form nearly complete sets in the subspaces spanned by all β values. In the deuteron a similar set of $0d$ states was also included. The parameters $V_1, V_2, V_3, V_4, a_1, a_2, a_3, a_4$, and $W + M$ were determined by fitting them simultaneously to the experimental g.s. energies and rms charge radii of d , t , and α and to the singlet s deuteron energy, while the weight of the d -state admixture of the deuteron was kept close to 4%. We included the triton in this fitting procedure to facilitate the use of the force in calculations involving any of the $0s$ clusters. It was after this procedure that the smaller

TABLE I. Width parameters of the basis functions.

	N	Width parameters (fm^{-2})
β	2	0.303, 0.646
$\gamma_{(pn)}$	9	0.0101, 0.0256, 0.0620, 0.147, 0.341, 0.757, 2.91, 6.51, 13.82
γ^a	6	0.0548, 0.1728, 0.32, 0.54, 1, 3.16

^aFor all relative motions except pn .

sets of α and deuteron size parameters for the cluster-model calculations (Table I) were determined by energy minimization. With the reduced dimensions adopted, the energy minima were shifted up by less than 20 keV.

The subsystem that depends neither on the tensor nor on the spin-orbit force but solely on the singlet-odd combination,

$$\omega = W + H - M - B, \quad (13)$$

is the 1P_1 wave of the $p+n$ scattering. The parameter ω was therefore fitted to the 1P_1 -wave $p+n$ phase shift. The last independent combination of the mixing parameters, of the central force, whose effect can be separated is [9]

$$\eta = 4W - M + 2B - 2H. \quad (14)$$

The subsystems affected by η are $\alpha+p$ and $\alpha+n$. The partial wave that is very sensitive to η (and is unaffected by the tensor interaction) is the p wave. To eliminate the effect of the the spin-orbit term as well, η was determined by fitting the weighted average of the calculated $p_{3/2}$ and $p_{1/2}$ $\alpha+p$ phase shifts to that of the experimental ones. The phenomenon that is most sensitive to the mixing parameters of the tensor force, the only parameters that are still undefined, is the the splitting between the 3P_J ($J = 0, 1, 2$) $p+n$ phase shifts. We thus adjusted W_T (and M_T) to this splitting.

The parameter values obtained are given in Table II. [For the exchange mixtures, see set (1).] The resulting g.s. properties of d , t , and α are compared with experiment in Table III. Although the agreement is acceptable, it is less satisfactory than what we obtained earlier with a purely central force [8, 9]. In particular, all free clusters are somewhat larger than they should be. The present model appears to be cruder because, for the cluster intrinsic motions, it is less consistent than the one

implied by the central force. The matter is that, while the constraint on the weight of the d -wave component of the deuteron forces the tensor interaction to play a substantial role in the deuteron binding, it is not allowed to contribute to the binding of the other clusters. It is, however, in agreement with the central forces used in the previous model that the present force binds the singlet deuteron.

What the central force cannot produce but the present one can is quadrupole moment. The deuteron quadrupole moment we obtained is $0.43 e \text{ fm}^2$, while the experimental value is $0.28 e \text{ fm}^2$. When the force is made artificially stronger so as to give the correct binding, the quadrupole moment reduces to $0.28 e \text{ fm}^2$, while the rms charge radius reduces to 2.138 fm. Thus these discrepancies are all interrelated.

The resulting phase shifts are qualitatively correct, but are not perfect. We only present the $p_{3/2}$ and $p_{1/2}$ $\alpha+n$ phase shifts, which are certainly the most important ones (Fig. 1). Although the spin-orbit coupling chosen [28] works well [30] in combination with another central force, and that is reproduced by our computer code, the same spin-orbit coupling does not give enough splitting in combination with our central force [with η of set (1) in Table II]. The two η values obtained by fitting to these phase shifts separately [sets (2) and (3) in Table II] reproduce the experiment better but still with a smaller accuracy than our earlier model with a purely central force [10].

B. The energy of ${}^6\text{Li}$

The interaction optimized for the subsystems according to Sec. III A [with exchange-parameter set (1)] puts the energy of the ${}^6\text{Li}$ g.s. at -30.923 MeV, which is to be compared with the experimental value, -31.994 MeV. The difference is of the order we obtained with central forces [8], and is of the correct sign, leaving space for the inclusion of further configurations to lower the theoretical energy. This lack of binding is somewhat larger than those found in the most realistic macroscopic three-particle models. Their binding energy with respect to the energy of the three-cluster dissociation threshold is typically 0.2–0.5 MeV too weak [11, 14, 31, 32].

TABLE II. Force parameters.

i	1	2	3	4	5
V_i (MeV)	105.16	-31.56	338.28	-3.54	-224.8
a_i (fm)	0.4	2.2	0.3	2.2	0.707
Exchange mixtures ^a		W	M	B	H
(1) η fitted to average of $p_{3/2}$, $p_{1/2}$ $\alpha+n$		0.4051	0.6386	-0.0425	-0.0012
(2) η fitted to $p_{3/2}$ $\alpha+n$; best for ${}^6\text{Li}$		0.4328	0.6109	-0.0148	-0.0288
(3) η fitted to $p_{1/2}$ $\alpha+n$		0.3697	0.6739	-0.0779	0.0342
(4) Artificial ^b		0.8474	0.1962	-0.5401	0.4964

^a $W_T = 0.3$, $M_T = 0.7$.

^b ω changed to produce a large $(S, L) = (0, 1)$ component in ${}^6\text{Li}$, η refitted to the ${}^6\text{Li}$ energy.

TABLE III. Energies (in MeV) and rms radii (in fm) of the free clusters. These properties are independent of the exchange mixture η . Weight of the d -wave component of the deuteron state equals 4.11%.

	E^d	r^d	$E_{(S=0)}^d$	E^t	r^t	E^α	r^α
Theory	-2.203	2.341	-0.976 ^a	-8.389	1.959	-28.306	1.740
Experiment	-2.225	2.095	-0.066 ^b	-8.482	1.70	-28.296	1.674

^aBound state.

^bAntibound state.

What is lacking in the ${}^6\text{Li}$ binding energy in models of either type is due to cluster *three-body* effects, which are not of the same nature though. The difference lies in the three-cluster effects caused by breathing distortions and by Pauli exchanges. Both of these effects are included only in the microscopic model, thus their contribution must arise as a departure from experiment only in the predictions of the macroscopic model.

The contribution of the breathing distortion of the α cluster can be calculated by comparing the binding energy of the distortion model with that of a “frozen” model. This involves a truncation of the basis, which can be realized by taking Eq. (6), rather than (7), as the trial function. We performed this calculation with exchange-parameter set (2), which is optimal for the $p_{3/2}$ $\alpha + n$ phase shift and yields a ${}^6\text{Li}$ energy, $E_{\alpha\text{Li}} = -32.043$ MeV, close to the experimental value. (This is not the best set deduced from the subsystems because it is far from optimum for the $p_{1/2}$ phase shift.) As Table IV shows, the α distortion in ${}^6\text{Li}$ causes a gain of 0.109 MeV in the binding energy. This indicates that the (breathing) distortion of the α particle constitutes only a small fragment of the distortion effects. In Table IV are shown also the binding energies of ${}^5\text{He}$, calculated in analogous models in a pseudobound-state approximation [33]. The difference between the full and frozen models is 0.007 MeV. This shows that the breathing distortion effects in

${}^6\text{Li}$ cannot be obtained by adding up those coming from the individual nucleons, so they are largely *three-body* effects. Since the interactions used in the macroscopic models are fitted to the properties of the two-body subsystems, they only bear the small two-body distortions, thus part of the missing binding energy must be caused by the three-body breathing distortions.

The effect of the three-body Pauli exchanges is a more obscure point. The effective three-body force arising from Pauli exchanges has been shown to depend strongly on the off-shell behavior of the *two-body* intercluster forces [34]. Thus their contribution to the binding energy also depends on the off-shell behavior of the two-cluster forces, which is not known for the interactions used in the macroscopic models. If their effect is some additional Pauli exclusion, their contribution may be expected to be repulsive, and so their neglect probably pushes the energy of the three-cluster system downwards. This may explain why the macroscopic model lacks a smaller fraction of the ${}^6\text{Li}$ binding energy.

All three-body effects other than the Pauli effects are bound to be attractive since they can be included in the microscopic model by extending the model state space. The most prominent of these is probably the $t + \tau$ admixture in the ${}^6\text{Li}$ wave function. It is an intriguing question whether they are able to yield the missing 1 MeV contribution to the binding.

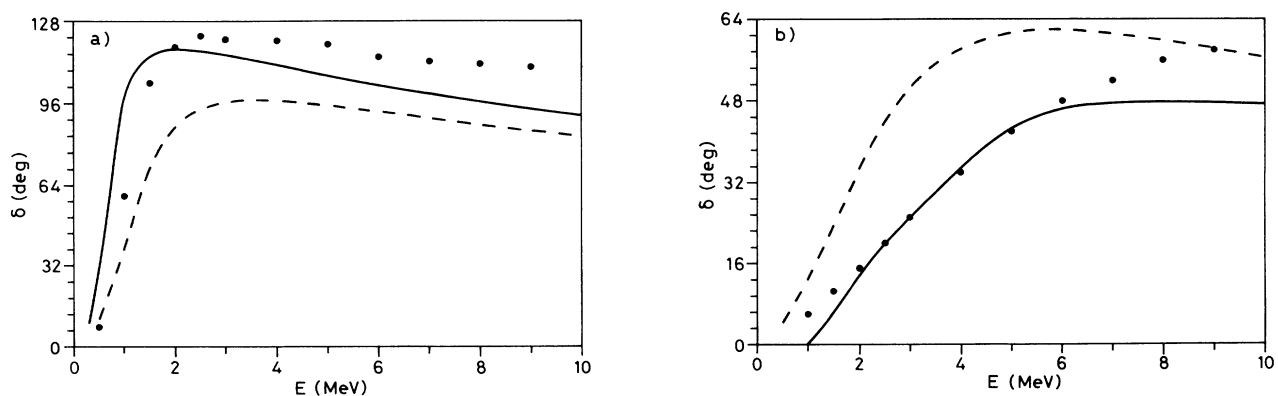


FIG. 1. Experimental [29] and theoretical (a) $p_{3/2}$ and (b) $p_{1/2}$ phase shifts. The dashed lines result from calculations with η fitted to their average [set (1) in Table II], while the full lines are results with two η 's fitted to $p_{3/2}$ and $p_{1/2}$ separately [sets (2) and (3) in Table II].

TABLE IV. Energies of the ${}^5\text{He}$ and ${}^6\text{Li}$ g.s. in MeV with the force fitted to the subsystems [set (2) in Table II].

	$E_{s_{\text{He}}}$	$E_{s_{\text{He}}} - E_{\alpha}$	$E_{s_{\text{Li}}}$	$E_{s_{\text{Li}}} - E_{\alpha}$
Full model	-27.354 ^a	0.952	-32.043	-3.737
Frozen model	-27.347 ^a	0.959	-31.934	-3.628
Experiment	-27.41	0.89	-31.994	-3.697

^aBound-state approximation.

IV. PROPERTIES OF ${}^6\text{Li}$

As was discussed in Ref. [9], no realistic estimates of the fragmentation properties are conceivable without the separation energies being correct. The most important one, the $\alpha + d$ separation energy can be made correct by changing the η value of the force. Set (2) of the exchange parameters (Table II) yields $E_{s_{\text{Li}}} = -32.043$ MeV (Table IV) and $E_{s_{\text{Li}}} - E_{\alpha} - E_d = -1.534$ MeV, and that is good enough since the experimental value is -1.47 MeV. Therefore, throughout this section, we used this set for ${}^6\text{Li}$.

A. Radius and quadrupole moment

The size of ${}^6\text{Li}$ reflects the puffiness of the free clusters, though it is inflated to a slightly lesser extent. The rms charge radius we obtained is 2.763 fm, while the experimental value is 2.56 fm [35]. The theoretical rms radius of the point matter density is 2.643 fm.

Although we do not attempt to solve the enigma of the quadrupole moment of ${}^6\text{Li}$ here, we have to state that our wave function yields $0.246 e \text{ fm}^2$, while the experimental value is $-0.064 e \text{ fm}^2$ [35]. This cannot be accounted for simply by the too-large deuteron quadrupole moment because the deuteron contraction in ${}^6\text{Li}$ [7] completely blurs the picture.

The ${}^6\text{Li}$ quadrupole moment has recently been reproduced fairly well by Unkelbach and Hofmann [36] as a result of an interplay between $(pn)\alpha$ configurations of $\{S, (l_1 l_2) L\} = \{1, (00)0\}$, $\{1, (20)2\}$, $\{1, (02)2\}$, and of the negligibly small configuration, $\{1, (22)2\}$. Since we chose to drop even the $\{1, (02)2\}$ component on account of its insignificance for the energy, we had to test the effect of this omission. Therefore, we temporarily restored this component, and got $0.229 e \text{ fm}^2$ for the quadrupole moment. The difference is so little, obviously, because the other clusterizations that overlap with this one do already represent it almost completely (cf. Sec. IV B). To seek further the cause of the discrepancy, we repeated the calculation in a model which only contains $(pn)\alpha$ configurations, with components $\{S, (l_1 l_2) L\} = \{1, (00)0\}$, $\{1, (20)2\}$, and $\{1, (02)2\}$. This model differs from that of Unkelbach and Hofmann [36] only in the tiny $\{1, (22)2\}$ component. The quadrupole moment was found to be $-0.18 e \text{ fm}^2$. This finding clearly shows how delicate the balance of the various effects is in the quadrupole moment. To check the role of the $\{1, (20)2\}$ component in this restricted model, we dropped it, with the result 0.297

$e \text{ fm}^2$ for the quadrupole moment. Thus we can confirm the significance of this component, along with several others, without being able to name definitely what is lacking from an agreement with experiment.

In a recent paper [37] Eramzhyan *et al.* report on a microscopic extension of the macroscopic three-cluster model of Kukulin *et al.* [14, 15, 20]. For the quadrupole moment they obtained a positive value, which is an order of magnitude larger than ours. To explain this failure, they propose that the d -state component of the α cluster in ${}^6\text{Li}$ may be important due to a polarizing distortion effect, and that may well be true.

B. Cluster ingredients

Before we show anything comparable with experimental data, it is important to relate the present approach to others and to assess the significance of the physical ingredients one by one. To this end, we have calculated the weights of various components and examined the effects of their omission. The present model improves on the earlier one [7–10] in that it contains noncentral force terms and the $(\alpha n) + p$ and $(\alpha p) + n$ clusterizations. We are therefore interested in the magnitude and role of angular-momentum mixing and of cluster-configuration mixing.

In Table V we show the weights of the different (S, L) components in the g.s. of ${}^6\text{Li}$, along with similar results of four macroscopic models. The state space of our former model [7–10] corresponds to the $(S, L) = (1, 0)$ subspace of this model, so the enormous extension of the basis now gives rise to new components of weights totalling 5.38%. Very slight though this may seem, such components may have appreciable effects.

All results agree in putting the weight of $(S, L) \neq (1, 0)$ at a few percent. A bifurcation can, however, be observed in the estimate for the amount of the $(S, L) = (0, 1)$ admixture: while three calculations give values around 4%, our calculation, in keeping with that of Kukulin *et al.* [14, 15], yields about 1%. The $(S, L) = (0, 1)$ component is fed by all three clusterizations with quantum numbers $(l_1, l_2) = (1, 1)$. It is plausible and has been corroborated by test calculations that the weight of this contribution depends crucially, and almost solely, on the singlet-odd

TABLE V. Decomposition of the g.s. of ${}^6\text{Li}$ into components of definite summed nucleon spin S and total orbital momentum L .

S, L	Lehman ^a	Bang ^b	Kukulin ^c	Danilin ^d	Micr. ^e
1,0	0.9178	0.928	0.9554	0.9304	0.9462
1,1	0.0050	0.007	0	0.0024	0.0020
1,2	0.0371	0.012	0.0338	0.0338	0.0391
0,1	0.0401	0.053	0.0108	0.0334	0.0127

^aReference [38], force given in [11].

^bReference [31], force given in [39].

^cReference [15], force given in [40].

^dReference [32], force given in [41].

^ePresent microscopic model; force: set (2) in Table II.

term of the nucleon-nucleon force, i.e., on the exchange parameter ω . The fit to the low-energy 1P_1 phase shift with our force is excellent (see Fig. 2), and so is it with the force [40] used in Ref. [15]. Thus the deviations appearing in other calculations must be caused either by the nucleon-nucleon force used or by the treatment of the $(0, 1)$ component. In particular, in the model of Lehman *et al.* [11] no singlet-odd nucleon-nucleon force term is included, whereas in the work of Bang and Gignoux [31] the $(0, 1)$ component is only included in the $(\alpha p)n$ and $(\alpha n)p$ partitions, possibly with some truncations [38]. We thus believe that the correct value of the weight of this component must be about 1%.

Nevertheless, for test purposes, we performed a calculation with an ω value that gives a large weight (0.0649) to this component. The modified parameters are dubbed “artificial” in Table II. The 1P_1 phase shift produced by this force is also shown in Fig. 2.

The presence of a type of clustering μ in the wave function Ψ is to be characterized by the weight of the component, of Ψ , that lies in the segment of the state space associated with that particular clusterization. This weight S_μ is called the amount of clustering [7], and is defined as the expectation value of the projection operator P_μ that projects onto the subspace μ :

$$S_\mu = \langle \Psi | P_\mu | \Psi \rangle. \quad (15)$$

The subspaces μ that we consider are those constituting the model space. Each bears a partition label, $(pn)\alpha_i$, $(\alpha_i p)n$, or $(\alpha_i n)p$, and a set of angular-momentum coupling labels $S, (l_1 l_2)L$. The calculable formula of S_μ is given in Appendix A.

The amounts of all clusterings represented explicitly in the basis of Eqs. (6) and (7) are given in Table VI. The most conspicuous feature of these data is that the values belonging to the same (S, L) but different partitions are surprisingly close to each other. Examining Table V, one can recognize that the major components $(S, L) = (1, 0)$, $(S, L) = (1, 2)$ are almost completely covered by the par-

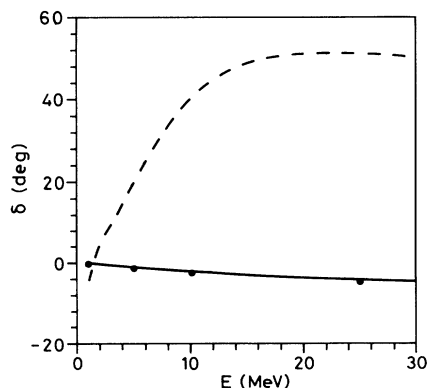


FIG. 2. 1P_1 $p+n$ phase shifts calculated with the optimized value of the mixing parameter ω (solid line) and with the artificially modified ω value [set (4) in Table II; dashed line]. Experiment: Ref. [42].

TABLE VI. Cluster decomposition of the g.s. of ^6Li . [Force: set (2) in Table II.]

Partition	Clusterization $S, (l_1 l_2)L$	Amount of clustering	
		$\alpha = \alpha_0$	$\alpha = \alpha_1$
$(pn)\alpha$	1,(00)0	0.9414	0.4614
$(pn)\alpha$	1,(20)2	0.0376	0.0002
$(pn)\alpha$	1,(02)2	0.0030 ^a	0.0006 ^a
$(pn)\alpha$	0,(11)1	0.0119	0.00005
$(\alpha p)n$	1,(11)0	0.8575	0.0254
$(\alpha p)n$	1,(11)1	0.0016 ^a	0.00006 ^a
$(\alpha p)n$	1,(11)2	0.0036	0.0003
$(\alpha p)n$	0,(11)1	0.0123	0.00008
$(\alpha n)p$	1,(11)0	0.8550	0.0252
$(\alpha n)p$	1,(11)1	0.0019	0.00008
$(\alpha n)p$	1,(11)2	0.0035	0.0003
$(\alpha n)p$	0,(11)1	0.0123	0.00008

^aOmitted from the basis. Sec. II.

tition $(pn)\alpha$. For example, the weight of the fraction, of the $(S, L) = (1, 0)$ subspace, that is not covered by the partition $(pn)\alpha_0$ is $0.9462 - 0.9414 = 0.0048$. The largest clusterizations $\{(pn)\alpha; 1, (00)0\}$, $\{(\alpha p)n; 1, (11)0\}$, and $\{(\alpha n)p; 1, (11)0\}$ overlap strikingly with each other, even more than in less sophisticated models [7], and some of the minor clusterizations are essentially identical with each other. The closeness of the basis to overcompleteness is also revealed by Table VII, which shows how little the energy is changed when any one of the clusterization components is excluded from the basis. (The components involving α_0 and α_1 are dropped simultaneously.) It is fascinating that when the main component, $\{(pn)\alpha; 1, (00)0\}$ is dropped, the energy is raised by a mere 0.65 MeV. Moreover, the amount of $\{(pn)\alpha_0; 1, (00)0\}$ clustering changes from 94.14% to just 93.60%.

The role of each individual clusterization component is seen better in Table VIII. This comprises the results of a series of calculations in which the number of clus-

TABLE VII. Change of the ^6Li g.s. energy when each one of the clusterization components is omitted. [Force: set (2) in Table II.]

Partition	Omitted component		Energy (MeV)
	$S, (l_1 l_2)L$		
	None		-32.043
$(pn)\alpha$	1,(00)0		-31.397
$(pn)\alpha$	1,(20)2		-30.500
$(pn)\alpha$	0,(11)1		-32.043
$(\alpha p)n$	1,(11)0		-32.010
$(\alpha p)n$	1,(11)2		-32.034
$(\alpha p)n$	0,(11)1		-32.037
$(\alpha n)p$	1,(11)0		-31.999
$(\alpha n)p$	1,(11)1		-31.956
$(\alpha n)p$	1,(11)2		-32.034
$(\alpha n)p$	0,(11)1		-32.038

TABLE VIII. Change of the energy and of the angular-momentum decomposition of the g.s. of ${}^6\text{Li}$ with a gradual elimination of the clusterizations. [Force: set (2) in Table II.]

Omitted component		Energy (MeV)	Weights of components (SL)			
Partition	$S, (l_1 l_2)L$		(10)	(11)	(12)	(01)
None		-32.043	0.9462	0.0020	0.0391	0.0127
$(\alpha p)n, (\alpha n)p$	1,(11)2	-31.982	0.9453	0.0021	0.0391	0.0135
$(\alpha p)n, (\alpha n)p$	0,(11)1	-31.940	0.9479	0.0023	0.0391	0.0107
$(\alpha n)p$	1,(11)1	-31.852	0.9491	0	0.0393	0.0116
$(\alpha p)n, (\alpha n)p$	1,(11)0	-31.732	0.9492	0	0.0399	0.0108
$(pn)\alpha$	0,(11)1	-31.574	0.9595	0	0.0405	0
$(pn)\alpha$	1,(20)2	-29.348	1	0	0	0

terizations included is decreased from all to one. The trial function resulting in the last line is contained in the subspace of the earlier model, $\{(pn)\alpha; 1, (00)0\}$ [7–10]. We see that the energy steps are very small except for the last one. This shows that the new model entails one major improvement, owing to the inclusion of the component $\{(pn)\alpha; 1, (20)2\}$, and a number of small ones. It is paradoxical that the $(\alpha p)n, (\alpha n)p$ clusterizations with $S, (l_1 l_2)L = 1, (11)0$ seem to play a much smaller role now than the more restrictive ${}^5\text{He}+p$ component, with $S, (l_1 l_2)L = 1, (11)0$ in an $\{\alpha + d, {}^5\text{He}+p\}$ model [27], which contributed to the binding by 0.6 MeV. The explanation is that the present $\{(pn)\alpha; 1, (00)0\}$ trial-function term is much more flexible than the αd term in Ref. [27], so that the $(pn)\alpha$ subspace contains a much larger fraction of the $(\alpha p)n, (\alpha n)p$ components of the wave function than the αd subspace contains of the ${}^5\text{He}+p$ component. The remarkable stability of the weights of the (S, L) subspaces against the omission of clusterizations up to the last one of those having a component in the particular (S, L) is again due to the large overlap of the different clusterizations.

C. Spectroscopic factors

1. Formulae

The spectroscopic factor of fragmentation into the two-body channel $c \equiv c_1 + c_2 \equiv (\bar{1}\bar{2}) + \bar{3}$ is the norm square of an amplitude function $g_c(\mathbf{r})$,

$$s_c = \int d\mathbf{r} |g_c(\mathbf{r})|^2, \quad (16)$$

defined as

$$g_c(\mathbf{r}) = \langle \Psi_{\mathbf{r}}^c | \Psi \rangle, \quad (17)$$

where $\Psi_{\mathbf{r}}^c$ is the antisymmetrized angular-momentum coupled product of the intrinsic wave functions of the fragments pinned down at a relative distance r . In the coupling scheme $[(I_1 S_2)I, l_2]J$ the function $\Psi_{\mathbf{r}}^c$ is given by

$$\Psi_{\mathbf{r}}^c = \mathcal{A} \left\{ [[\Phi_{c_1(I_1)} \phi_{c_2(S_2)}]_I \delta_{l_2}(\mathbf{r} - \boldsymbol{\rho}_2)]_J \right\}, \quad (18)$$

where

$$\delta_{lm}(\mathbf{r} - \boldsymbol{\rho}) = r^{-2} \delta(r - \rho) Y_{lm}(\hat{\rho}). \quad (19)$$

The label c_1 is understood to contain all labels written explicitly in Eq. (8) and not summed over in Eq. (9) or in (10):

$$\Phi_{c_1(I_1)} = \sum_{\text{mixing}} \mathcal{A} \left\{ \left[\phi_{(\bar{1}\bar{2})(S_1)} \tilde{\chi}_{l_1}^{\bar{1}\bar{2}}(\boldsymbol{\rho}_1) \right]_{I_1} \right\}, \quad (20)$$

where the summation goes over l_1 and over the α states $\bar{1}$ when $\bar{1} + \bar{2} = p + n$ and when $\bar{1} + \bar{2} = \alpha + n$, respectively.

The spectroscopic amplitude is in fact an overlap between two three-cluster states. It is therefore usual to express it in terms of overlaps between the generator-coordinate basis states involved in the cluster model. However, owing to the delta function in (18), it is not trivial to find such an expression. The standard method involves integral transformations [25]. We avoided these at the expense of a matrix diagonalization. To our knowledge, our method is new, and we present it in Appendix B.

2. Results

We are interested in $\alpha + d$ and ${}^5\text{He}+p$ spectroscopic factors. The results are summarized in Table IX.

The $\alpha + d$ spectroscopic factor in the model of Lehman *et al.* [12] with 0% and with 4% deuteron d -state admixtures is 0.632 and 0.654, respectively. The former value is modified to 0.847 by Pauli corrections [21], so a similar correction on the latter value may be expected to yield some 0.87. This is in full accord with our present estimate, 0.883. The reduction from ~ 0.93 to 0.883 should primarily be due to a broader spread of the ${}^6\text{Li}$ wave function on the complete set of states of the $\alpha + d$ system. The only other appreciable cause may be a size mismatch between the free deuteron and the deuteron in ${}^6\text{Li}$. The larger the free deuteron, the more the deuteron cluster is contracted in ${}^6\text{Li}$ [7] and the smaller the overlap is between them. Thus our too-large deuteron may cause the spectroscopic overlap to be too small. The α cluster being, on the contrary, rigid, its size in ${}^6\text{Li}$ [7] cannot differ too much from that of the free α particle. To test the effect of the deuteron size, we constructed a deuteron of rms radius 2.138 fm (and of energy -2.230 MeV, d -state weight 4.1%, and quadrupole moment 0.28 e fm 2 ; see Sec. III A) by an *ad hoc* modification of the

TABLE IX. Spectroscopic factors $s_{[(I_1, S_2)I, l_2]J}^{(\bar{1}2)\bar{3}}$ of the decomposition of ${}^6\text{Li}$.

Model	$s_{[(10)1,0]1}^{d\alpha}$	$s_{[(3/2,1/2)1,1]1}^{5\text{He}p} + s_{[(3/2,1/2)2,1]1}^{5\text{He}p}$	$s_{[(1/2,1/2)0,1]1}^{5\text{He}p} + s_{[(1/2,1/2)1,1]1}^{5\text{He}p}$
$(pn) + \alpha, l_1 = l_2 = 0^a$	0.930	0.436	0.283
$(pn) + \alpha, l_1 = l_2 = 0^b$	0.930	0.415	0.280
$\alpha + p + n^c$	0.883	0.044+0.456=0.500	0.113+0.241=0.354
$\alpha + p + n^d$		0.015+0.406=0.421	0.093+0.337=0.430

^aComputed with the shifted Gaussian bases and force of Refs. [7, 10].

^bComputed with the force of Ref. [7] and with changing-width h.o. bases, as in the present model.

^cForce: set (2) in Table II.

^dForce artificially modified to yield a large component of $S = 0, L = 1$; set (4) in Table II.

force. The spectroscopic amplitude calculated with this deuteron yields almost the same, $s^{d\alpha}=0.901$.

The amplitude functions belonging to these two values of the spectroscopic factor are compared with that of Ref. [7] in Fig. 3. The node position depends apparently just on the cluster sizes. For instance, the node of the dotted line (the present ${}^6\text{Li}$ with the well-sized deuteron) is shifted outwards with respect to the dashed line (taken from Ref. [7]) because of the oversized α particle of the present model. The rather large value of the asymptotic normalization constant, $\bar{C}_{\alpha d} = 3.75$, belonging to the solid curve fits into a simple trend of cluster-size dependence [9], too. The prediction of the $(pn)\alpha$ model of $l_{pn} = l_{d\alpha} = 0$ with an interaction that sets the cluster sizes correct is about 3.2 [9]. We deem this to be a more realistic estimate. Nevertheless, the fact that the present model gives rise to no reduction makes one suspect that the disagreement [9] with the experimental value, 2.15 ± 0.06 [43], is likely to survive any extension of the $\alpha + p + n$ relative-motion space.

The nucleus ${}^5\text{He}$ being unbound, the ${}^5\text{He}+p$ spectroscopic factor is to be defined as a continuous function of the ${}^5\text{He}$ energy (“differential spectroscopic factor” [10]). The $(pn)\alpha$ model with $l_{pn} = l_{d\alpha} = 0$ overshoots the tran-

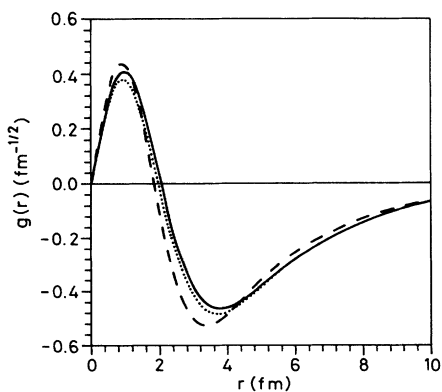


FIG. 3. Alpha+deuteron spectroscopic amplitudes calculated in our present model ($s^{d\alpha} = 0.883$, solid line), with the same ${}^6\text{Li}$ wave function but with a deuteron of the correct size ($s^{d\alpha} = 0.901$, dotted line) and in the earlier $(pn)\alpha$ model with $l_{pn} = l_{d\alpha} = 0$ of Ref. [7] ($s^{d\alpha} = 0.929$, dashed line).

sitions found in the ${}^6\text{Li}(e, e'p)$ experiment as well as in the macroscopic model [17] beyond the peak due to the $p_{3/2}$ resonance in the $\alpha + n$ channel [10]. (The agreement is much better beyond the $t + d$ threshold, where the structure of ${}^5\text{He}$ is dominated by the $t + d$ component [44, 10]). In the region of the discrepancy the transition goes predominantly to the $p_{1/2}$ $\alpha + n$ state, although the contribution of the $p_{3/2}$ $\alpha + n$ wave is also significant. The discrepancy is thus to be expressed as a disagreement in the spectroscopic factors pertinent to the ${}^5\text{He}$ quantum numbers $(S_{\alpha n}, l_{\alpha n})I_{\alpha n} = (\frac{1}{2}, 1)\frac{3}{2}$ and $(\frac{1}{2}, 1)\frac{1}{2}$.

For the description of the $\frac{3}{2}^-$ and $\frac{1}{2}^-$ states of ${}^5\text{He}$ we used the exchange-parameter sets (2) and (3), respectively, in Table II. Since we can compute continuum wave functions only in the shifted Gaussian representation [10], we computed the ${}^5\text{He}+p$ spectroscopic factor in the pseudobound-state approximation [10], with a basis that produces the correct resonance energy [33]. The values obtained in this way should correspond to single resonances. They are thus somewhat smaller than the integrals of the spectroscopic factors over the whole region of our interest, but they closely follow the tendency of the integrated spectroscopic factors from one model to the other. We can thus infer from the bound-state estimates for the behavior of the differential spectroscopic factors.

The values calculated in the present approach for the model of Ref. [10] (line 2 in Table IX) differ slightly from those of Ref. [10] (line 1) mainly because the way in which the tail of the pseudobound $\alpha + n$ wave function is cut off is specific to the relative-motion basis. In line 3 we see that by introducing the improvements entailed by the present model the spectroscopic factors are enhanced, whereby the discrepancy with respect to experiment is bound to become even larger.

We can thus conclude that, despite earlier expectations [10], the enlargement of the ${}^6\text{Li}$ model space does not improve the ${}^5\text{He}+p$ spectroscopic factor. We still have to clarify, however, an even more unnerving aspect of the differences from the predictions [17] of the model of Lehman *et al.* In Sec. IV B we have found that the only prominent difference in the ${}^6\text{Li}$ wave function between the two models was in the weight of the $(S, L) = (0, 1)$ component. In Ref. [10] we conjectured that the macroscopic model owes its success in producing the correct

${}^5\text{He}+p$ spectroscopic factor just to this component. In Sec. IV B we have, however, established with some confidence that the correct weight of this term should not be as large as that. Is it thus possible that the macroscopic model gives so satisfactory results due to a defect? The answer is fortunately negative. As the last line of Table IX reveals, the artificial enhancement of the weight of this component does not improve the spectroscopic factor at all.

To sum up, the inclusion of all small terms, whether they are realistic or overestimated, does not cause any qualitative change. Thus the origin of the discrepancy is to be found in circumstances common to the old model [10] and the present one.

V. CONCLUSION

We have rigorously implemented the viewpoint of the microscopic cluster approach to the most perfect existing representative of nuclear three-cluster systems, the g.s. of ${}^6\text{Li}=\alpha+p+n$. That there is room for improvement on the earlier models, at least in one respect, was shown by the success of the macroscopic three-cluster approach. We wanted to eliminate a flaw of our earlier microscopic model of the same breed or wanted to know the limits of the microscopic multicluster approach. The results seem to realize the latter alternative.

The philosophy of the microscopic cluster approach allows the cluster internal motions to be described essentially as single-particle motions. The improvement introduced now consists in the inclusion of noncentral force terms and an extension of the intercluster relative-motion state space to embrace three-cluster dynamics more completely. We sought an interaction that describes the subsystems and applied it to the three-cluster model. The description of the subsystems turns out to be less perfect now than with the more primitive pure central force obviously because the more realistic treatment of the $p+n$ system now is not consistent with the description of the α particle in a space of 0s Slater determinants. Nevertheless, the force optimized for the subsystems requires only a minor correction to set the ${}^6\text{Li}$ energy right.

The model ${}^6\text{Li}$ so obtained is slightly oversized, and its quadrupole moment, small as it is, has the wrong sign. Test calculations revealed that by trimming the state space, one can easily reverse the sign. A recent reproduction of the quadrupole moment with a smaller state space [36] thus needs confirmation by calculations with an extended state space.

The flaw of the previous approach was its inability to reproduce the ${}^5\text{He}+p$ spectroscopic factor, and the present model fails to improve on it. We have now shown that this problem is unrelated to the truncation of the relative-motion space or to the neglect of any angular-momentum components. To clarify its origin, we recall [10] the sum rule which states that the sum of the spectroscopic factors of the removal of a proton from ${}^6\text{Li}$ with any angular momentum and with the residual five-nucleon system left behind in any state is 3. The sum rule is model independent in the sense that its deriva-

tion only requires quantum mechanics; thus our models strictly observe it, and, presumably, so does nature to a good approximation. The fact that the calculated value is larger than the experimental one in the $\alpha+n$ energy region below 17.6 MeV [10] implies that somewhere at higher energies their relation must be reversed. So the behavior of the theoretical value may be interpreted as a "distortion of the $\alpha+n$ continuum" such that the excess of spectroscopic strength at low energies is compensated for by a lack of strength at higher energies. In this context it is appropriate to recall Fig. 1, which shows a similar compression effect for the $\alpha+n$ phases. (The change of the phase shift between energies zero and infinity is predetermined by Levinson's theorem in much the same way as the integral of the spectroscopic factor is set by the sum rule.) Such an effect was observable in the previous model [10] as well to a lesser extent, whereas the Lehman model [11] is certainly free of this defect. It is now plausible to relate the two observations, and infer that the discrepancy comes from the same defect of the interaction that causes the error in the $\alpha+n$ phase shift.

The quality of the p -wave fits is so mediocre because there is only a single parameter to control it, η . The interaction is constrained, to a great extent, by the state spaces assigned to the cluster internal motions. The macroscopic approach appears to be superior because it is free of such constraints. In the microscopic approach the constraint could be loosened by a force of more complicated functional form, but could only be eliminated entirely by abandoning the use of Slater determinants, which, however, entails formidable complications.

Attributing the failure in the ${}^5\text{He}+p$ spectroscopic factor to the inadequacy of the description of the $\alpha+n$ continuum, we can regain our confidence in the ${}^6\text{Li}$ wave function we obtained. The interaction can indeed be expected to work better for bound states because its geometrical and strength parameters were set to bound-state properties. Thus it is not surprising that the estimates for the $\alpha+d$ spectroscopic factor, ranging 0.88–0.90, are in full agreement with the Pauli-corrected [21] value derived from the macroscopic model [12].

By inclusion of partitions other than $(pn)\alpha$ we tested the adequacy of $(pn)\alpha$ bases commonly used in macroscopic models [14, 15, 20] as well as in microscopic ones. We have found that the $(\alpha n)p$ and $(\alpha p)n$ partitions add very little components to the wave function, which justifies the use of pure $(pn)\alpha$ bases. Although this conclusion is valid for the macroscopic approach as well, the true extent of its validity is revealed only at the microscopic level, where the tendency of antisymmetrization to make macroscopically different function spaces indistinct is manifest.

The only appreciable ($\gg 1\%$) $(S, L) \neq (1, 0)$ component we have found is the one with $[S, (l_{pn}l_{d\alpha})L] = [1, (20)2]$. This contradicts some of the macroscopic-model results, which put the $(S, L) = (0, 1)$ component at 3–5% [38, 31, 32]. We propose that the treatment of the singlet-odd component of the nucleon-nucleon relative motion used in these works is responsible for the discrepancy.

Of course, the details of the angular-momentum com-

position matters primarily in the electromagnetic form factors, which we did not consider in this paper. But understanding the correspondence with the macroscopic models better, one may now accept, with more confidence, the results obtained in the macroscopic model [19, 20] as authentic. For instance, the role of the $(S, L) = (0, 1)$ component in the electromagnetic properties can be tested in the macroscopic framework as well. What remains to be done in the *microscopic* model of ${}^6\text{Li}$ is to go beyond the $\alpha + p + n$ picture.

This research was supported by OTKA (National Science Research Foundation, Hungary) under Contract No. 3010.

APPENDIX A: COMPUTATION OF THE AMOUNT OF CLUSTERING

The terms (1) of the trial function (7) are constructed explicitly by substituting (4) into (1). Thus, the component of the trial function belonging to subspace $\nu = \{(12)3; S_\nu, (l_{\nu_1} l_{\nu_2})L_\nu\}$ can be written as

$$\Psi_{S_\nu, (l_{\nu_1} l_{\nu_2})L_\nu}^{(12)3} = \sum_{ii'} C_i C_{i'} \psi_{\nu ii'}, \quad (\text{A1})$$

where

$$\psi_{\nu ii'} = \mathcal{A} \left\{ \left[\Phi_{\nu(S_\nu)} [\Gamma_{il_{\nu_1}}^{(1)}(\rho_{\nu_1}) \Gamma_{i'l_{\nu_2}}^{(2)}(\rho_{\nu_2})]_{L_\nu} \right]_{JM} \right\}. \quad (\text{A2})$$

Each subspace ν is thus spanned by the nonorthogonal set of functions $\{\psi_{\nu ii'}\}$, so that

$$\Psi = \sum_{\nu ii'} F_{\nu ii'} \psi_{\nu ii'}. \quad (\text{A3})$$

The coefficients $F_{\nu ii'}$ result from the nuclear-structure calculation.

The amount of two-cluster clustering spanned by a

$$\begin{aligned} \Psi_{\mathbf{r}}^c = \sum_{\text{mixing}} (-1)^{I_1 - I - S_1} [(2I_1 + 1)(2I + 1)]^{1/2} \sum_{S, L} (-1)^S [(2S + 1)(2L + 1)]^{1/2} W(l_1 S_1 I S_2; I_1 S) W(S l_1 J l_2; I L) \\ \times \mathcal{A} \left\{ \left[\phi_{c_1(S_1)} \phi_{c_2(S_2)} \right]_S [\tilde{\chi}_{l_1}^{\bar{1}\bar{2}}(\rho_1) \delta_{l_2}(\mathbf{r} - \rho_2)]_J \right\}, \end{aligned} \quad (\text{B1})$$

where W are Racah coefficients. This being substituted into (17), yields

$$\begin{aligned} g_c(\mathbf{r}) = \sum_{\text{mixing}} (-1)^{I_1 - I - S_1} [(2I_1 + 1)(2I + 1)]^{1/2} \sum_{S, L} (-1)^S [(2S + 1)(2L + 1)]^{1/2} W(l_1 S_1 I S_2; I_1 S) W(S l_1 J l_2; I L) \\ \times \sum_{\nu} \delta_{L_\nu L} \delta_{S_\nu S} \langle \tilde{\chi}_{l_1}^{\bar{1}\bar{2}}, \mathbf{r} | \hat{A}_{\mu\nu} | \chi_{l_{\nu_1}}^{12}, \chi_{l_{\nu_2}}^{(12)3} \rangle, \end{aligned} \quad (\text{B2})$$

where the ternary clusterization μ underlying the binary fragmentation c is specified by $\mu = \{(\bar{1}\bar{2})\bar{3}; S, (l_1 l_2)L\}$, and the matrix element has been written with the Dirac convention observed. Thus $|\mathbf{r}\rangle$ stands for the eigenvector, belonging to eigenvalue \mathbf{r} , of the spatial coordinate of the second variable of the *abstract* operator $\hat{A}_{\mu\nu}$.

To show the method of expressing $g_c(\mathbf{r})$ in terms of $N_{\mu ii'; \nu jj'}$, we need not carry along all subscripts. The expressions

particular nonorthogonal basis in a state given as a superposition of similar clusterizations has been derived in Ref. [7] [Eq. (3.10)]. That formula can be generalized to multicluster clusterings included explicitly in a multi-cluster basis. An application of that formula to a three-cluster clustering μ of the present type gives

$$\begin{aligned} \mathcal{S}_\mu = \sum_{\nu \rho} \sum_{ii' jj' kk' ll'} F_{\nu ii'}^* N_{\nu ii'; \mu jj'} \\ \times [N_{\mu\mu}]_{(jj'); (kk')}^{-1} N_{\mu kk'; \rho ll'} F_{\rho ll'}, \end{aligned} \quad (\text{A4})$$

where

$$N_{\mu ii'; \nu jj'} = \langle \psi_{\mu ii'} | \psi_{\nu jj'} \rangle \quad (\text{A5})$$

$$= \langle \Gamma_{il_{\mu_1}}^{(1)} \Gamma_{i'l_{\mu_2}}^{(2)} | \hat{A}_{\mu\nu} | \Gamma_{jl_{\nu_1}}^{(1)} \Gamma_{j'l_{\nu_2}}^{(2)} \rangle, \quad (\text{A6})$$

with $\hat{A}_{\mu\nu}$ being an integral operator, whose kernel is the overlap

$$\begin{aligned} A_{\mu\nu}(\mathbf{r}_1, \mathbf{r}_2; \mathbf{r}'_1, \mathbf{r}'_2) \\ = \left\langle \mathcal{A} \left\{ \left[\Phi_{\mu(S_\mu)} [\delta_{l_{\mu_1}}(\mathbf{r}_1 - \rho_{\mu_1}) \delta_{l_{\mu_2}}(\mathbf{r}_2 - \rho_{\mu_2})]_{L_\mu} \right]_J \right\} \right| \\ \times \left| \mathcal{A} \left\{ \left[\Phi_{\nu(S_\nu)} [\delta_{l_{\nu_1}}(\mathbf{r}'_1 - \rho_{\nu_1}) \delta_{l_{\nu_2}}(\mathbf{r}'_2 - \rho_{\nu_2})]_{L_\nu} \right]_J \right\} \right\rangle. \end{aligned} \quad (\text{A7})$$

The matrix elements $N_{\mu ii'; \nu jj'}$ are nothing but the overlaps between the elements of the basis, and are always available since they are computed in the first step of the structure calculation.

APPENDIX B: SPECTROSCOPIC AMPLITUDE FORMULA

The function $\Psi_{\mathbf{r}}^c$ in (18) can be cast into a form showing a semblance of our three-cluster state by inserting (20) in it and recoupling the angular momenta as follows:

$$g(\mathbf{r}) = \langle \mathbf{r} | \hat{A} | \chi \rangle, \quad (\text{B3a})$$

$$s = \int d\mathbf{r} \langle \chi | \hat{A} | \mathbf{r} \rangle \langle \mathbf{r} | \hat{A} | \chi \rangle = \langle \chi | \hat{A}^2 | \chi \rangle \quad (\text{B3b})$$

can be trivially identified with single terms of (B2) and of the corresponding expression for the spectroscopic factor, respectively. ($\hat{A} = \langle \tilde{\chi}_{l_1}^{\bar{1}\bar{2}} | \hat{A}_{\mu\nu} | \chi_{l_{\nu_1}}^{12} \rangle$, etc.) It thus remains to show how to express these two quantities in terms of

$\langle \tilde{\Gamma}_i | \hat{A} | \Gamma_j \rangle$, where $\tilde{\Gamma}_i, \Gamma_j$ are functions of the type of (5).

Let us solve the eigenvalue equation of the positive definite matrix $\langle \tilde{\Gamma}_i | \tilde{\Gamma}_j \rangle$:

$$\sum_j \langle \tilde{\Gamma}_k | \tilde{\Gamma}_j \rangle c_j^{(i)} = a_i c_k^{(i)}. \quad (\text{B4})$$

Due to the orthonormality of the eigenvectors,

$$\sum_k c_k^{(i)*} c_k^{(j)} = \delta_{ij}, \quad (\text{B5})$$

the single-particle state vectors

$$|i\rangle = a_i^{-1/2} \sum_j c_j^{(i)} |\tilde{\Gamma}_j\rangle \quad (\text{B6})$$

also form an orthonormal set. If the set $\{\tilde{\Gamma}_j\}$ is chosen so as to cover the spatial region of physical interest fully enough, then $\{|i\rangle\}$ can be taken as an approximately complete and exactly orthonormal set, so that

$$1 \approx \sum_i |i\rangle \langle i| = \sum_i a_i^{-1} \sum_{jk} c_j^{(i)} |\tilde{\Gamma}_j\rangle \langle \tilde{\Gamma}_k | c_k^{(i)*}. \quad (\text{B7})$$

Inserting this in front of \hat{A} in (B3a) and in between the two operators \hat{A} implicit in the extreme right of (B3b), we obtain

$$\begin{aligned} g(\mathbf{r}) &\approx \sum_{ijkl} a_i^{-1} c_j^{(i)} \tilde{\Gamma}_j(\mathbf{r}) c_k^{(i)*} \langle \tilde{\Gamma}_k | \hat{A} | \Gamma_l \rangle F_l \\ &= \sum_{ijkl} a_i^{-1} c_j^{(i)} \tilde{\Gamma}_j(\mathbf{r}) c_k^{(i)*} N_{kl} F_l, \end{aligned} \quad (\text{B8a})$$

$$\begin{aligned} s &\approx \sum_{ijklm} F_i^* \langle \Gamma_i | \hat{A} | \tilde{\Gamma}_k \rangle c_k^{(j)} a_j^{-1} c_l^{(j)*} \langle \tilde{\Gamma}_l | \hat{A} | \Gamma_m \rangle F_m \\ &= \sum_{ijklm} F_i^* (N^\dagger)_{ik} c_k^{(j)} a_j^{-1} c_l^{(j)*} N_{lm} F_m, \end{aligned} \quad (\text{B8b})$$

where $|\chi\rangle = \sum_i F_i |\Gamma_i\rangle$ and $N_{ij} = \langle \tilde{\Gamma}_i | \hat{A} | \Gamma_j \rangle$. It is reasonable to choose the single-particle bases $\{\tilde{\Gamma}_i\}$ and $\{\Gamma_j\}$ to be the same as $\{\Gamma_{i\mu_2}^{(2)}\}$ and $\{\Gamma_{j\nu_2}^{(2)}\}$ used in the structure calculation for the μ and ν components, respectively. In this way the matrix elements N_{ij} and coefficients F_i correspond to $N_{\mu i i'; \nu j j'}$ and $F_{\nu i i'}$, respectively. Thus the only extra calculation needed is the solution of the trivial eigenvalue problem (B4).

We note that, unlike the integral transformation techniques, this method does contain some approximation, which is, however, just a repeated application of the approximation underlying the solution of the nuclear-structure problem. The present method is related to the exact techniques in the same way as the method used for the calculation of the amount of clustering is [7]. Test calculations for the $\alpha + d$ spectroscopic factor show that the result agrees with the exact value to a great accuracy.

It should also be noted that we had introduced a series expansion method for the calculation of the potential overlap earlier [45], and that proved to be inaccurate. Its inaccuracy was caused by the fact that a non-antisymmetric function was expanded in terms of antisymmetric ones [46]. The present method is free of such defects, and it could be applied to the calculation of the potential overlap as well.

-
- [1] Y. Fujiwara, H. Horiuchi, K. Ikeda, M. Kamimura, K. Katō, Y. Suzuki, and E. Uegaki, *Prog. Theor. Phys. Suppl.* **68**, 29 (1980); H. Furutani, H. Kanada, T. Kaneko, S. Nagata, H. Nishioka, S. Okabe, S. Saito, T. Sakuda, and M. Seya, *ibid.* **68**, 193 (1980).
- [2] R. Krivec and M. V. Mihailović, *J. Phys. G* **8**, 821 (1982).
- [3] R. Beck, F. Dickmann, and A. T. Kruppa, *Phys. Rev. C* **30** 1044 (1984); H. Kanada, T. Kaneko, S. Saito, and Y. C. Tang, *Nucl. Phys.* **A444**, 209 (1985).
- [4] P. H. Wäckman and N. Austern, *Nucl. Phys.* **30**, 529 (1962).
- [5] K. Hahn, E. W. Schmid, and P. Doleschall, *Phys. Rev. C* **31**, 325 (1985).
- [6] In Refs. [2–5] we restricted ourselves to works on the $\alpha + p + n$ system.
- [7] R. Beck, F. Dickmann, and R. G. Lovas, *Ann. Phys. (N. Y.)* **173**, 1 (1987).
- [8] A. T. Kruppa, R. G. Lovas, R. Beck, and F. Dickmann, *Phys. Lett. B* **179**, 317 (1986).
- [9] R. G. Lovas, A. T. Kruppa, R. Beck, and F. Dickmann, *Nucl. Phys.* **A474**, 451 (1987).
- [10] R. G. Lovas, A. T. Kruppa, and J. B. J. M. Lanen, *Nucl. Phys.* **A516**, 325 (1990).
- [11] D. R. Lehman, M. Rai, and A. Ghovanlou, *Phys. Rev. C* **17**, 744 (1978).
- [12] D. R. Lehman and M. Rajan, *Phys. Rev. C* **25**, 2743 (1982).
- [13] W. C. Parke and D. R. Lehman, *Phys. Rev. C* **29**, 2319 (1984).
- [14] V. I. Kukulin, V. M. Krasnopol'sky, V. T. Voronchev, and P. B. Sazonov, *Nucl. Phys.* **A417**, 128 (1984).
- [15] V. I. Kukulin, V. M. Krasnopol'sky, V. T. Voronchev, and P. B. Sazonov, *Nucl. Phys.* **A453**, 365 (1986).
- [16] R. Ent, H. P. Blok, J. F. A. van Hienen, G. van der Steenhoven, J. F. J. van den Brand, J. W. A. den Herder, E. Jans, P. H. M. Keizer, L. Lapikás, E. N. M. Quint, P. K. A. de Witt Huberts, B. L. Berman, W. J. Briscoe, C. T. Christou, D. R. Lehman, B. E. Norum, and A. Saha, *Phys. Rev. Lett.* **57**, 2367 (1986).
- [17] J. B. J. M. Lanen, A. M. van den Berg, H. P. Blok, J. F. J. van den Brand, C. T. Christou, R. Ent, A. G. M. van Hees, E. Jans, G. J. Kramer, L. Lapikás, D. R. Lehman, W. C. Parke, E. N. M. Quint, G. van der Steenhoven, and P. K. A. de Witt Huberts, *Phys. Rev. Lett.* **62**, 2925 (1989).
- [18] A. T. Kruppa, R. Beck, and F. Dickmann, *Phys. Rev. C* **36**, 327 (1987).
- [19] A. Eskandarian, D. R. Lehman, and W. C. Parke, *Phys. Rev. C* **38**, 2341 (1988).
- [20] V. I. Kukulin, V. T. Voronchev, T. D. Kaipov, and R. A. Eramzhyan, *Nucl. Phys.* **A517**, 221 (1990).
- [21] K. Varga and R. G. Lovas, *Phys. Rev. C* **43**, 1201 (1991).

- [22] Y. Fujiwara and Y. C. Tang, *Phys. Lett.* **131B**, 261 (1983).
- [23] $\mathcal{A} = n^{-1/2} \sum_1^n (-1)^P P$, where P runs over all of the n intercluster permutations.
- [24] Y. Suzuki, *Prog. Theor. Phys.* **50**, 341 (1973).
- [25] H. Horiuchi, *Prog. Theor. Phys. Suppl.* **62**, 90 (1977).
- [26] G. F. Filippov, V. S. Vasilevski, and L. L. Chopovski, *Fiz. Elem. Chastits At. Yadra* **15**, 1338 (1984) [*Sov. J. Part. Nucl.* **15**, 600 (1984)].
- [27] R. Beck, F. Dickmann, and R. G. Lovas, *Nucl. Phys.* **A446**, 703 (1985).
- [28] I. Reichstein and Y. C. Tang, *Nucl. Phys.* **A158**, 529 (1970).
- [29] R. A. Arndt and L. D. Roper, *Phys. Rev. C* **1**, 903 (1970).
- [30] G. Blüge and K. Langanke, *Phys. Rev. C* **41**, 1191 (1990).
- [31] J. Bang and C. Gignoux, *Nucl. Phys.* **A313**, 119 (1979).
- [32] B. V. Danilin, M. V. Zhukov, A. A. Korshennikov, and L. V. Chulkov, *Yad. Fiz.* **53**, 71 (1991).
- [33] R. G. Lovas and M. A. Nagarajan, *J. Phys. A* **15**, 2383 (1982).
- [34] S. Nakaichi-Maeda and E. W. Schmid, *Z. Phys. A* **318**, 171 (1984).
- [35] F. Ajzenberg-Selove, *Nucl. Phys.* **A413**, 1 (1984).
- [36] M. Unkelbach and H. M. Hofmann, *Few-Body Systems* **11**, 143 (1991).
- [37] R. A. Eramzhyan, V. I. Kukulin, G. G. Ryzhikh, and Yu. M. Tchuvilsky, Australian National University Report No. ANU-ThP-3/92 (1992).
- [38] D. R. Lehman and W. C. Parke, *Few-Body Systems* **1**, 193 (1986).
- [39] R. de Tournell, B. Rouben, and D. W. L. Sprung, *Nucl. Phys.* **A242**, 445 (1975).
- [40] R. V. Reid, *Ann. Phys. (N. Y.)* **50**, 411 (1968).
- [41] D. Gogny, P. Pires, and R. de Tournell, *Phys. Lett.* **32B**, 591 (1970).
- [42] R. A. Arndt, R. H. Hackman, and L. D. Roper, *Phys. Rev. C* **15**, 1002 (1977).
- [43] M. P. Bornand, G. R. Plattner, R. D. Viollier, and K. Alder, *Nucl. Phys.* **A294**, 492 (1978).
- [44] J. B. J. M. Lanen, R. G. Lovas, A. T. Kruppa, H. P. Blok, J. F. J. van den Brand, R. Ent, E. Jans, G. J. Kramer, L. Lapikás, E. N. M. Quint, G. van der Steenhoven, P. C. Tiemeijer, and P. K. A. de Witt Huberts, *Phys. Rev. Lett.* **63**, 2793 (1989).
- [45] R. G. Lovas, K. F. Pál, and M. A. Nagarajan, *Nucl. Phys.* **A402**, 141 (1983).
- [46] R. G. Lovas and K. F. Pál, *Nucl. Phys.* **A424**, 143 (1984).